arXiv:1405.7825v1 [hep-ph] 30 May 2014

Non-Abelian Bremsstrahlung and Azimuthal Asymmetries in High Energy p+A Reactions

M. Gyulassy,[1,2,*] P. Levai,[1] I. Vitev,[3] and T. Biro[1]

[1] *MTA WIGNER Research Centre for Physics, RMI, Budapest, Hungary*
[2] *Department of Physics, Columbia University, New York, NY 10027, USA*
[3] *Theoretical Division, Los Alamos National Laboratory, Los Alamos, NM 87545, USA*

(Dated: May 30, 2014)

We apply the GLV reaction operator solution to the Vitev-Gunion-Bertsch (VGB) boundary conditions to compute the all-order in nuclear opacity non-abelian gluon bremsstrahlung of event-by-event fluctuating beam jets in nuclear collisions. We evaluate analytically azimuthal Fourier moments of single gluon, $v_n^M\{1\}$, and even number 2ℓ gluon, $v_n^M\{2\ell\}$ inclusive distributions in high energy p+A reactions as a function of harmonic n, target recoil cluster number, M, and gluon number, 2ℓ, at RHIC and LHC. Multiple resolved clusters of recoiling target beam jets together with the projectile beam jet form Color Scintillation Antenna (CSA) arrays that lead to characteristic boost non-invariant trapezoidal rapidity distributions in asymmetric $B+A$ nuclear collisions. The scaling of intrinsically azimuthally anisotropic and long range in η nature of the non-abelian bremsstrahlung leads to v_n moments that are similar to results from hydrodynamic models, but due entirely to non-abelian wave interference phenomena sourced by the fluctuating CSA. Our analytic non-flow solutions are similar to recent numerical saturation model predictions but differ by predicting a simple power-law hierarchy of both even and odd v_n without invoking k_T factorization. A test of CSA mechanism is the predicted nearly linear η rapidity dependence of the $v_n(k_T,\eta)$. Non-abelian beam jet bremsstrahlung may thus provide a simple analytic solution to Beam Energy Scan (BES) puzzle of the near $\sqrt{s}$ independence of $v_n(p_T)$ moments observed down to 10 AGeV where large-x valence quark beam jets dominate inelastic dynamics. Recoil bremsstrahlung from multiple independent CSA clusters could also provide a partial explanation for the unexpected similarity of v_n in $p(D)+A$ and non-central $A+A$ at same $dN/d\eta$ multiplicity as observed at RHIC and LHC.

PACS numbers: 24.85.+p; 12.38.Cy; 25.75.-q

I. INTRODUCTION

An unexpected discovery at RHIC/BNL in $D+Au$ reactions at $\sqrt{s}=200$ AGeV [1] and at LHC/CERN in $\sqrt{s}=5.02$ ATeV $p+Pb$ reactions [2–4] is the large magnitude of mid-rapidity azimuthal anisotropy moments, $v_n(k_T,\eta=0)$, that are remarkably similar to those observed previously in non-central $Au+Au$ [5–7] and $Pb+Pb$ [8–12] reactions. See preliminary data in Fig. 1 taken from ATLAS [13] Fig. 24 that also shows a large rapidity-even dipole v_1 harmonic[14].

In addition, the Beam energy Scan (BES) at RHIC [15] revealed a near $\sqrt{s}$ independence from 8 AGeV to 2.76 ATeV of the v_n in $A+A$ at fixed centrality that was also unexpected.

In high energy $A+A$, the v_n moments have been interpreted as possible evidence for the near "perfect fluidity" of the strongly-coupled Quark Gluon Plasmas (sQGP) produced in such reactions [16–20]. However, the recent observation of similar v_n in much smaller $p(D)+A$ systems and also the near beam energy independence of the $A+A$ moments observed in the Beam Energy Scan (BES) [15] at RHIC together with LHC, from 7.7 AGeV to 2.76 ATeV have posed a problem for the perfect fluid interpretation because near inviscid hydrodynamics is

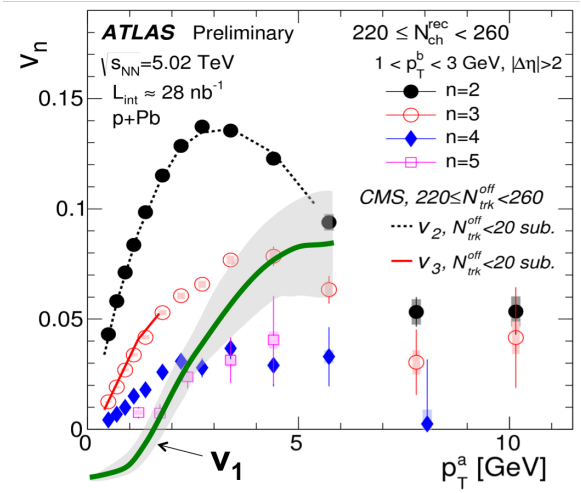

FIG. 1: (Color online) Reproduced from ATLAS [13] p+Pb Figure 24 $v_n(p_T)$ with n=2 to 5 obtained for $|\Delta\eta|>2$ and the p_T range of 1-3 GeV. An overlay sketch of preliminary rapidity-even v_1 data shown at QM14 [14] is also indicated. The error bars and shaded boxes represent the statistical and systematic uncertainties, respectively. Results in $220 N_{ch}<260$ are compared to the CMS data [2] obtained by subtracting the peripheral events (the number of offline tracks $N_{off}^{trk}<20$), shown by the solid and dashed lines.

**gyulassy@phys.columbia.edu

not expected to apply in space-time regions where the local temperature falls below the confinement temperature, $T(x,t) < T_c \sim 160$ MeV. In that Hadron Resonance Gas (HRG) "corona" region, the viscosity to entropy ratio is predicted to grow rapidly with decreasing temperature [21] and the corona volume fraction must increase relative to the ever shrinking volume of the perfect fluid "core" with $T > T_c$ when either the projectile atomic number A and size $A^{1/3}$ fm or the center-of-mass (CM) energy $\sqrt{s}$ decrease .

While hydrodynamic equations have been shown to be sufficient to describe $p(D) + A$ data with particular assumptions about initial and freeze-out conditions [22], its necessity as a unique interpretation of the data is not guaranteed. This point was underlined recently using a specific initial state saturation model [23] that was shown to be able to fit $p(D) + A$ correlation even v_n moments data without final state interactions. That saturation model has also been used [19] to specify initial conditions for perfect fluid hydrodynamics in $A+A$. However, in $p + A$ such initial conditions for hydrodynamics are not as well-controlled because the gluon saturation scale scale, $Q_s(x, A = 1) < 1$ GeV, is small and its fluctuations in the transverse plane on sub-nucleon scales are not reliably predicted.

The near independence of v_n moments on beam energy observed in BES [15] at RHIC from 7.7 AGeV to 2760 AGeV pose further serious challenges to the uniqueness of the perfect fluid interpretations of the data because of previous predictions [24] for systematic reduction of the moments due to the increasing HRG corona. Those predictions appeared to be confirmed by SPS $\sqrt{s} = 17$ AGeV data [25]. The most recent BES measurements, however, appear to contradict the diluting role of the HRG corona. The HRG corona fraction should dilute perfect fluid QGP core flow signatures at lower energies unless additional dynamical mechanisms possibly associated with increasing baryon density accidentally conspire to compensate for growing HRG corona fraction. Such combination of canceling effects with $\sqrt{s}$ was demonstrated to be possible using a specific hybrid hydro+URQMD model [27] or three fluid models [28]. While such hybrid models are *sufficient* to explain the BES independence of v_2 data in $A + A$, the *necessity* and, hence, uniqueness of such hybrid descriptions are not guaranteed.

The BES [15] data also pose a challenge to color glass condensate (CGC) gluon saturation model [19] used to specify initial conditions for hydrodynamic flow predictions in $A + A$. This is because Q_s^2 is predicted to decrease with $\log(s)$, and thus gluon saturation-dominated high energy gluon fusion models of initial-state dynamics should switch over into valence quark-diquark dominated inelastic dynamics when partons with fractional energy $x > 0.01$ play the dominant role. At RHIC and lower energies valence quark and diquark QCD string phenomenology based on the LUND [52] model with (diquark-quark) beam jets and its $B + A$ nuclear collision generalization via HIJING [38] can smoothly interpolate between AGS and RHIC energies. Such multiple beam jet based approach to $B + A$ naturally accounts, for example, for the striking long range triangular, boost non-invariant, form of $(dN_{pA}/d\eta)/(dN_{pp}/d\eta)$ nuclear enhancement of the final hadron rapidity density in $p(D) + A$ observed at all CM energies up to LHC [32]. By including multiple mini and hard jet production it can account for the $\sqrt{s}$ growth of $dN_{B+A}/d\eta$ though at top $\sqrt{s} = 200$ AGeV RHIC and at LHC energies there is strong evidence for the onset for gluon saturation [33] that limits $2 \to 2$ minijet processes to $p_T > Q_s(x, A) \propto A^{1/3}/x^{\lambda}$ that grows with A and $1/x = \sqrt{s}/(p_T e^{\eta})$.

The importance of multiple beam jets with rapidity kinematics controlled by valence quarks and diquarks was first proposed within the Brodsky-Gunion-Kuhn (BGK) model [30] which is reproduced also in the HIJING [31] model. The trapezoidal boost non-invariant dependence of the local density, $dN/d\eta d^2\mathbf{x}$, predicted in [31] as a function of the transverse coordinate $\mathbf{x}$ even in symmetric $A+A$, may also play an important role in in the triangular long range η dependence of $v_2(\eta, \sqrt{s})$ as observed in $Au+Au$ by PHOBOS [34].

In this paper we explore the possibility that a dynamical source that could partially account for the above puzzling azimuthal moment systematics may be traced to a basic perturbative QCD (pQCD) feature. The pQCD based model here extends the opacity $\chi = 1$ Gunion-Bertsch [35] (GB) perturbative QCD bremsstrahlung used to model for $\pi + \pi \to g + X$ to all orders in opacity, $e^{-\chi}\sum_{n=1}^{\infty}\chi^n/n!\cdots$, Vitev-Gunion-Bertsch (VGA) multiple interaction pQCD bremsstrahlung for applications to $B + A$ nuclear collisions. We show that VGA bremsstrahlung naturally leads on an event by event basis to a hierarchy of non trivial azimuthal asymmetry moments similar to those observed in $p + A$ (see fig.1) and peripheral $A + A$ at fixed $dN/d\eta$ [9, 11, 12] .

A particularly important feature of beam jet non-abelian bremsstrahlung is that it automatically leads to long range rapidity η "ridge" correlations and to all even and odd azimuthal $v_n\{2\ell\}$ harmonics with $n, \ell = 1, 2, 3, \cdots$. Conventional Lund string beam jet models [52], as encoded e.g. in HIJING, on the other hand neglect recoil induced moderate p_T color bremsstrahlung azimuthal asymmetries. From the pQCD perspective, beam jets are simply arrays of parallel color antennas that radiate due to multiple soft transverse momentum transfers $|\mathbf{q}_i| \sim 1$ GeV between participant projectile and $i = 1, \cdots, N_T(b)$ target nucleons. Many event generators include ϕ *averaged* (azimuthally randomized) bremsstrahlung effects via $\sim \alpha_s/k_T^2$ up to the minijet scale $k_T < Q_s(x, A)$. In HIJING the ARIADNE [54] code is used in conjunction with the non-perturbative Lund string fragmentation code JETSET [53] to incorporate this effect, while highly azimuthally asymmetric hard pQCD jets with $k_T > Q_s(x, A)$ are included via the PYTHIA [53]) code. In [52] it was emphasized that the high string tension of color strings reduces greatly the sensitivity of Lund string fragmentation to

QCD bremsstrahlung , and that this is an important infrared safety feature of that non-perturbative hadronization phenomenology.

In $p+A$ multiple collisions, however, the projectile accumulates multiple transverse momentum kicks (the Cronin effect) from scattering with cold nuclear participants [39, 49] that enhances the bremsstrahlung mean square $< k_T^2 >_{pA} \approx A^{1/3}\mu^2$ via random walk in the target frame. In the CGC approach this $A^{1/3}$ growth is built into $Q_s^2(x,A)$ in the infinite momentum frame.

At the minijet scale the underlying azimuthal asymmetry of non-abelian bremsstrahlung will tend to focus gluons toward the azimuthal directions of exchanged momenta. At present, this basic azimuthal dependence is not taken into account in HIJING.

As we show below, there is a very important aspect to the multiple color antenna arrays in high energy $p+A$ due to the longitudinal coherence of clusters of participant target beam jets separated by small transverse coordinates too small to be resolved by the transverse momenta involved. While the total average number of Glauber participant nucleons that interact with a projectile at impact parameter $\mathbf{b}$ is determined by the area of the inelastic cross section $\sigma_{in}(s) \sim$ few fm^2 as $N_T(\mathbf{b}) = \sigma_{in}(s)\int dz \rho_T(z,\mathbf{b})$, for moderate momentum transfers with $k_T \sim Q_s \sim$ 1-2 GeV bremsstrahlung the target participant antennas naturally group event by event into $M \leq N_T$ resolved clusters separated in the transverse plane by sub-nucleon distances $1/k_T \sim 0.2$ fm, similar to the CGC model [47] and in AdS/CFT shock modeling [48] of $p+A$, but here simply to transverse resolution scale of multiple scattering recoil kinematics in the target frame versus the infinite momentum frame.

This partial decoherence of the $N_T(b)$ participating target dipoles creates non-isotropic spatial distributions of color antennas that radiate according to the fluctuating spatial asymmetries from even to event. Each cluster is characterized by the number m_a of target participant dipole antennas that exchange coherently $Q_a^2 = m_a\mu^2$ with the projectile at a specific azimuthal angle ψ_a controlled by the transverse geometrical distribution of the clusters.

Each recoil cluster $a = 1, \cdots, M$ radiates coherently into a broad range of rapidities that appears in two particle correlations as $M+1$ "ridge" components with $\mathbf{k}$ near the cluster accumulated recoil transverse momenta $-\mathbf{Q}_a = -\sum_{i\in I_a}\mathbf{q}_i$ and with $\mathbf{k}$ near the projectile dipole (cluster) radiates near the total momentum transfer received $\mathbf{Q}_0 = (Q_0,\psi_0) = \sum_{a=1}^{M}\mathbf{Q}_a$. On an event-by-event basis M and the color antenna geometry fluctuate producing naturally $n = M+1$ and other azimuthal harmonics in two gluon $v_n = \langle\cos(n(\phi_1-\phi_2))\rangle$.

Our goal here is to estimate analytically the magnitude of the color bremsstrahlung source of pQCD dynamical azimuthal two particle correlations and its dependence of n, k, M, N_T. We illustrate the results with specific analytic cluster geometric limits, including Z_n symmetric and Gaussian random CSA. We propose a future generalization of HIJING that could enable more realistic testing the influence of anisotropic VGA bremsstrahlung on the final hadron flavor dependent azimuthal moments and competing minijet and hard jet sources of anisotropies.

II. FIRST ORDER IN OPACITY (GB) BREMSSTRAHLUNG AND AZIMUTHAL ASYMMETRIES v_n

The above puzzles with BES [15], $D+Au$ at RHIC, and with $p+Pb$ at LHC motivate us to consider an alternative, more basic, perturbative QCD source of azimuthal asymmetries.The well known non-abelian bremsstrahlung Gunion-Bertsch (GB) formula [35] for the soft gluon radiation single inclusive distribution is

$$\frac{dN_g^1}{d\eta d^2\mathbf{k} d^2\mathbf{q}} = \frac{C_R\alpha_s}{\pi^2}\frac{\mu^2}{\pi(q^2+\mu^2)^2}\frac{\mathbf{q}^2}{\mathbf{k}^2(\mathbf{k}-\mathbf{q})^2} \ , \quad (1)$$

where we characterize the parton scattering elastically with the cross section $d\sigma_0/d^2\mathbf{q} = \sigma_0\mu^2/\pi(q^2+\mu^2)^2$ off color neutral target participants with a momentum transfer $\mathbf{q}$ in terms of a characteristic cold nuclear matter scale $\mu^2 \approx 0.12$ GeV^2 taken from fits to forward dihadron correlations in [43–45]. Here $q = |\mathbf{q}|$ and the produced gluon has rapidity η and transverse momentum $\mathbf{k}$ ($k = |\mathbf{k}|$) in the final state. It is obvious from Eq. 1 that non-abelian gluon bremsstrahlung is preferentially emitted along two directions specified by the beam "$\hat{\mathbf{z}}$" axis and the transverse momentum transfer vector $\mathbf{q}$. The uniform rapidity-even, $\eta \approx \log(xE/k)$, distribution associated with moderate $\mathbf{q}$ scattering is a unique feature of non-abelian bremsstrahlung in the kinematic $k \ll xE \ll E$ range of interest associated with beam jets and is due to the triple gluon vertex. The uniform rapidity-even distribution is an especially important characteristic of non-abelian radiation. The combination of the two leads to a uniform rapidity "ridge" in the direction of the momentum transfer $\mathbf{q}$ that fluctuates in both magnitude and direction from event-to-event but measurable in two or higher gluon correlation measurements. The rapidity-even bremsstrahlung ridge is of course kinematically limited to $\eta \in [Y_T, Y_P]$ interval between the target and projectile rapidities. Independent but kinematically correlated multiple target and projectile beam jet bremsstrahlung sources can also naturally account for the triangle boost non-invariant rapidity density observed in $p+A$ as emphasized in Ref.[31].

For scattering of color neutral dipoles considered in [35] the Rutherford perturbative α^2/q^4 distribution of momentum transfers were modeled by color neutral form factors of the form $q^2(q^2+\mu^2)^{-1}$. For GB radiation the $\mathbf{k} = \mathbf{q}$ singularity is also regulated by such a form factors. Therefore the color neutralization scale μ^2 also regulates the $(\mathbf{k}-\mathbf{q})^2$ singularity in Eq. 1 as well. That x and A dependence of that scale arises naturally in small x models based the gluon saturation scale $Q_s(x,A)$ [46, 47, 50].

Our emphasis here however is to explore the general characteristics of $g+g \to g$ from the perturbative QCD perspectives that allows us to derive analytically many of the observed remarkably simple scaling relations between 2ℓ azimuthal harmonic cumulants, $v_n(2\ell)$, as a basic coherent state semi-classical wave interference effect without invoking hydrodynamic local equilibrium assumptions.

The screened single inclusive GB perturbative gluon distribution is

$$\frac{dN_g^{(1)}}{d\eta d^2\mathbf{k} d^2\mathbf{q}} \equiv f(\eta,\mathbf{k},\mathbf{q}) = \frac{C_R\alpha_s}{\pi^2 k^2}\frac{\mu^2 q^2}{\pi(q^2+\mu^2)^2}\frac{P_\eta}{(\mathbf{k}-\mathbf{q})^2+\mu^2} \quad (2)$$

$$\equiv \frac{F\ P}{A-\cos(\phi-\psi)} \quad (3)$$

where ϕ is the azimuthal angle of $\mathbf{k}$ and ψ is the azimuthal angle of $\mathbf{q}$ and abbreviations

$$A \equiv A_{kq} \equiv (k^2+q^2+\mu^2)/(2k\ q) \geq 1 \quad (4)$$

$$F \equiv F_{kq} \equiv \frac{C_R\alpha_s}{\pi^2 k^2}\frac{\mu^2 q^2}{\pi(q^2+\mu^2)^2}\frac{1}{2kq} \quad (5)$$

$$P \equiv P_\eta \equiv (1-e^{Y_T-\eta})^{n_f}(1-e^{\eta-Y_P})^{n_f} \ , \quad (6)$$

were introduced a kinematic rapidity envelope factor P_η corresponding to approximately uniform rapidity dependence of the non-abelian bremsstrahlung [35] regulated with $(1-|x_F|)^{n_f}$ kinematic spectator power counting [36, 46]. Note $n_f = 2n_{spec}-1 \sim 4$ for gluon production from the scattering of two color neutral dipoles in the large $|x_F| \to 1$ limit. The P_η rapidity envelopes can be used to build up multi beam jet boost non-invariant triangular $dN_{pA}/d\eta$ as in the BGK [30] model and also to model the intrinsic boost non-invariance of $dN_{AA}/d\eta d\mathbf{x}_\perp$ even in symmetric A+A collisions as with HIJING [31].

The single gluon azimuthal moments, $v_n = v_n\{1\}$ in cumulant notation, from a single GB color antenna defined by the momentum transfer $\mathbf{q} = (q,\psi)$ with azimuthal angle ψ are defined by

$$v_n^{GB}(k,q,\psi)f_0(k,q) = F\ P\int\frac{d\phi}{2\pi}\frac{\cos(n\phi)}{A-\cos(\phi-\psi)}$$

$$= F\ P\,\mathrm{Re}\oint_{|z|=1}\frac{dz}{2\pi i}\frac{(-2e^{in\psi})z^n}{(z^2-2Az+1)}$$

$$= F\ P\,\mathrm{Re}\,\frac{2(e^{i\psi}\ z_-)^n}{z_+-z_-} \ , \quad (7)$$

where we defined $z \equiv \exp(i(\phi-\psi))$, so that $d\phi = -idz/z$ and $\cos(\phi-\psi) = (z+1/z)/2$. Note that there are two simple real poles $z_\pm = A \pm \sqrt{A^2-1}$. Since $A \geq 1$, only z_- contributes to the unit contour integral, resulting in the final analytic expression above. Note that the azimuthal averaged single gluon inclusive ($n=0$) bremsstrahlung distribution with $v_0 = 1$ is then

$$f_0 = 2F\ P/(z_+-z_-) = F_{kq}P_\eta/(A_{kq}^2-1)^{1/2}$$

$$\propto dN/d\eta dk^2 dq^2 \ . \quad (8)$$

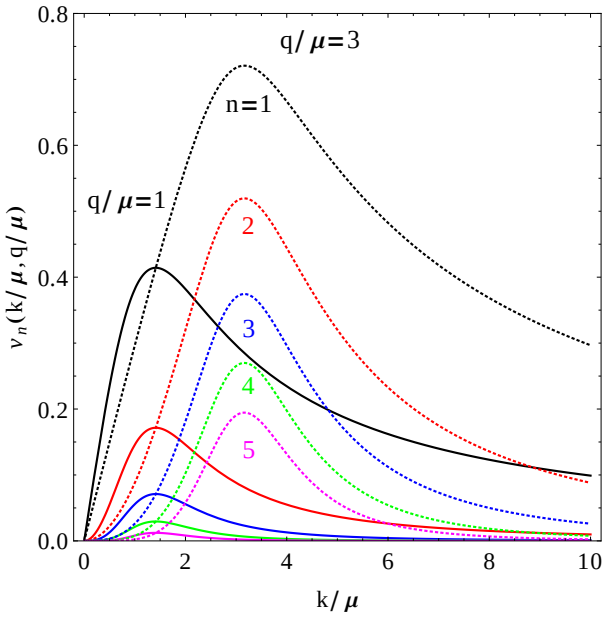

FIG. 2: (Color online) Single GB beam jet bremsstrahlung azimuthal Fourier moments, $v_n^{GB}(k/\mu, q/\mu)$ from Eq. (12) are shown versus k/μ for $n = 1-5$ for $q/\mu = 1(3)$ solid(dashed).

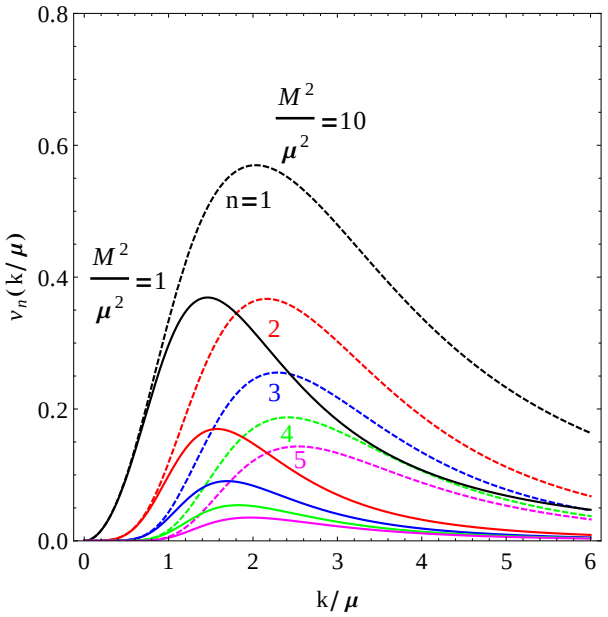

FIG. 3: (Color online) Single GB beam jet bremsstrahlung azimuthal Fourier moments, $\langle v_n^{GB}(k/\mu)\rangle$, averaged over q with $M^2/(q^2+M^2)^2$ are shown versus k/μ for $n = 1-5$ for $(M/\mu)^2 = 1$ (10) solid(dashed).

This has a collinear divergence at $k=q$ in the $\mu=0$ limit in addition to the usual abelian beam axis $1/k^2$ divergence. The first is regulated by the color neutral dipole form factor in the GB model.

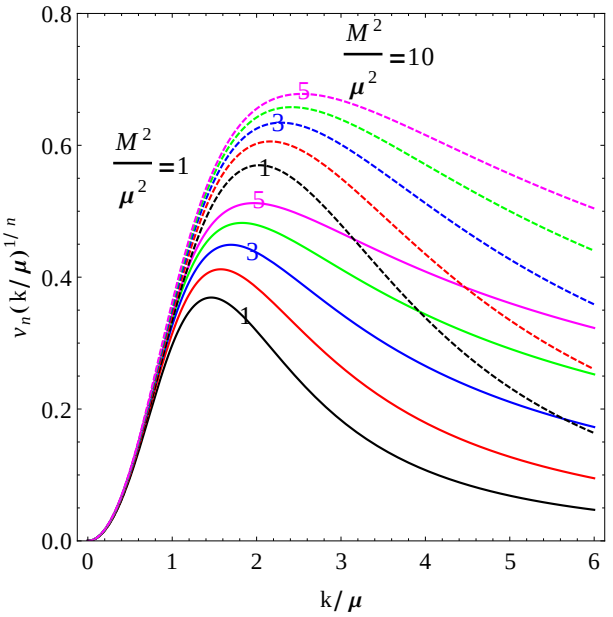

FIG. 4: (Color online) Ideal $1/n$ power scaling of q averaged $\langle v_n^{GB}(k/\mu)\rangle^{1/n}$ with $k \lesssim M$ (see Eq.11) breaks down at higher k because in the $M = 0$ limit of non-abelian bremsstrahlung limits $k \leq q$ (see Eq. (8)).

The azimuthal Fourier moments are however finite in Eq. (7) even in the case of vanishing μ and depend analytically on n and A via

$$v_1^{GB}(k,q,\psi) = \cos[\psi](A_{kq} - \sqrt{A_{kq}^2 - 1}) \quad (9)$$

$$\lim_{\mu\to 0} v_1^{GB}(k,q,0) = (k/q)\,\theta(q-k) \quad (10)$$

$$v_n^{GB}(k,q,\psi) = \cos[n\psi]\,(v_1^{GB}(k,q,0))^n \quad (11)$$

$$\lim_{\mu\to 0} v_n^{GB}(k,q,0) = (k/q)^n\,\theta(q-k)\ . \quad (12)$$

Note that in the $\mu = 0$ limit, all $v_n \to 1$ reach unity at $k = q$ but vanish for $k > q$. For finite $\mu > 0$, all moments maximizing at $k^2 = k_*^2 = q^2+\mu^2$ with $v_n(k_*) = (\sqrt{(1+\mu^2/q^2)}-\mu/q)^n$. Figure 2 illustrates the magnitude of GB $v_n(k/\mu, q/\mu)$ moments as a function of k/μ for $n = 1, \cdots, 5$ and two different $q/\mu = 1, 3$.

Note the remarkable power law scaling with n (for fixed $k, q.\psi$) of the azimuthal moments of gluon bremsstrahlung from a single GB color antenna:

$$[v_n^{GB}(k,q,0)]^{1/n} = [v_m^{GB}(k,q,0)]^{1/m}\ , \quad (13)$$

that is similar to the scaling observed by ALICE, CMS and ATLAS [4, 8, 11] at LHC at least for the higher $n \geq 3$ moments dominated by purely geometric fluctuations. This scaling is of course not expected to hold perfectly for ensemble q averaged ratios of $\cos(n\Delta\phi)$ of di-hadron inclusive rates. One of our aims below is to test the survival of the above ideal scaling in Eq. (13) to ensembles averages in two gluon inclusive processes.

However, note that by rotation invariance all harmonics $n > 0$ vanish for *single* inclusive GB antennas when averaged over the momentum transfer azimuthal angle ψ. We show below in section V that the finite *rms* fluctuating harmonics of *two particle* inclusive $(\langle\cos(n\Delta\phi)\rangle)^{1/2}$ survive with similar magnitude and k dependence as in Figs. 1,2.

In Fig. 4 we see that the simple fixed q power law scaling of Eqs. (11,13) holds for $k/M < 1$ but gradually breaks down at higher $k > M$ when ensemble averaged over q^2 in $\langle f_n(k)\rangle$.

III. ALL ORDERS IN OPACITY VGB GENERALIZATION OF GUNION-BERTSCH RADIATION

A recursive reaction operator method was originally developed in GLV [37, 38] to compute final-state multiple collision-induced gluon bremsstrahlung and elastic collisional energy loss [39] to all orders in opacity for applications to jet quenching. Extensions of the method to final state heavy quarks jet energy loss was given in [40, 41].

Vitev further extended the reaction operator method to compute non-abelian energy loss in cold nuclear matter in Ref. [42]. In addition to Final-State (FS) bremsstrahlung , Vitev solved the cold matter Initial-State (IS) bremsstrahlung problem to all orders in opacity and also the generalization of the first order in opacity Gunion-Bertsch [35] non-abelian bremsstrahlung problem to all orders in opacity for asymptotic ($t_0 \to -\infty, t_f \to +\infty$) boundary condition. We refer here to the Vitev all-order in opacity generalized GB radiation solution as VGB.

In [42] the VGB solution was regarded to be of mainly academic interest, since the focus there was on induced initial state IS and final state FS gluon bremsstrahlung associated with hard processes in $p + A$ [43–45]. In this paper, we focus entirely on the application of the VGB solution to low to moderate transverse momentum $k <$ few GeV gluon radiation from multiple beam jets in the same spirit as in GB [35], where the aim was to understand the general qualitative characteristics of inelastic high energy single inclusive processes from low order perturbative QCD perspective.

Our aim here is to calculate azimuthal asymmetry moments, $v_n(\eta, \mathbf{k})$, arising from basic perturbative QCD bremsstrahlung effects in high energy p+A interactions. The physical picture approximates p+A scattering as the scattering of an incoming color dipole at an impact parameter, $\mathbf{b}$, of high (positive) rapidity $Y_P \gg 1$ with $N_T^{part} \sim A^{1/3}$ nuclear target participant nucleons with high (negative) $Y_T \ll -1$ in the CM. The target participant dipoles at a fixed transverse coordinate $\mathbf{R}$ are separated longitudinal separations $\Delta z_i = z_i - z_{i-1} \sim$ fm in the cold nucleus target rest frame. However they act coherently when emitting gluons near mid rapidity due to Lorentz contraction in the CM and long formation time

of gluons $\sim [2\cosh(\eta)]/k$ in the lab frame.

However, the target participants are distributed in the transverse direction by transverse separations $R_{ij} = |\mathbf{R}_i - \mathbf{R}_j| \lesssim \sqrt{\sigma_{in}/\pi} \sim$ fm which can be resolved for $k > 1$ GeV. This leads incoherent groups of target nucleons that radiate mid-rapidity gluons with $|\eta| < 1$, $k > 1$ GeV gluons coherently. We propose in section IV below a simple percolation model to estimate the partially coherent target recoil bremsstrahlung . However, we concentrate in this section on the coherent projectile bremsstrahlung contribution.

The complete all orders in opacity, $\chi \equiv \chi(\mathbf{b}) = \int dz \sigma_g(z)\rho(z,\mathbf{b})$, VGB solution derived by Vitev in [42] is

$$\frac{dN^{VBG}}{d\eta d^2\mathbf{k}} = \sum_{n=1}^{\infty} \frac{dN_n^{VBG}}{d\eta d^2\mathbf{k}} = \frac{C_R\alpha_s}{\pi^2} \sum_{n=1}^{\infty} \left[\prod_{i=1}^{n} \int \frac{d\Delta z_i}{\lambda_g(z_i)}\right] \left[\prod_{j=1}^{n} \int d^2\mathbf{q}_j \left(v_j^2(\mathbf{q}_j) - \delta^2(\mathbf{q}_j)\right)\right] \times \mathbf{B}_{21}^b \cdot \left[\mathbf{B}_{21}^n + 2\sum_{i=2}^{n} \mathbf{B}_{(i+1)i}^n \cos\left(\sum_{j=2}^{i} \omega_{jn}\Delta z_j\right)\right] , \quad (14)$$

where the transverse vector "antenna" amplitudes $\mathbf{B}_{jk}^n$ are defined in terms of differences between"cascade" vector amplitudes $\mathbf{C}_{jn}$ as

$$\mathbf{B}_{jk}^n = \mathbf{C}_{jn} - \mathbf{C}_{kn} \quad (15)$$

$$\mathbf{C}_{jn} = \frac{\mathbf{k} - \mathbf{q}_j - \cdots - \mathbf{q}_n}{(\mathbf{k} - \mathbf{q}_j - \cdots - \mathbf{q}_n)^2} = \frac{\mathbf{k} - \mathbf{Q}_{jn}}{(\mathbf{k} - \mathbf{Q}_{jn})^2} \ . \quad (16)$$

Indices j, k, n here keep track of combinations of non-vanishing momentum transfers $\mathbf{q}_i$ from direct versus virtual diagrams contributing at a given opacity order n of the opacity expansion. The partial summed momentum transfers are $\mathbf{Q}_{jn} = \sum_{i=j}^{n} \mathbf{q}_i$ being the singular directions of non-abelian bremsstrahlung that also control the inverse formation times

$$\omega_{jn} = \frac{(\mathbf{k} - \mathbf{Q}_{jn})^2}{2E_g} \, . \quad (17)$$

Here $E_g = xE_P \ll E_P$ is the energy of the gluon in a frame where the energy of the proton projectile is assumed to be large $E_P \gg m_n$.

There are two simple limits depending on the kinematic range of interest. In the fully coherent limit, where $n\omega_{jn}\lambda_g \ll 1$, we can approximate all the cosines by unity. This is the limit we are interested in for our present applications to mid-rapidity multi-particle production not too close to projectile and target fragmentation regions, i.e $Y_T + 1 < \eta < Y_P - 1$.

The target scattering centers are ordered in this VGB problem as $z_0 = -\infty < z_1 < \cdots < z_n < z_f = +\infty$ with $\Delta z_i = (z_i - z_{i-1})$ for $i \geq 2$. $\sigma_g(z)\rho(z,\mathbf{b})$ is the local inverse mean free path of a gluon the nuclear target at position z impact parameter $\mathbf{b}$ in the target rest frame. The $v^2(\mathbf{q}_j) = \frac{d\sigma_{el}(z_j)}{d^2\mathbf{q}_j}$ denote normalized distributions of transverse momentum transfers at scattering center z_j.

In the coherent scattering limit of relevance to near mid-rapidity radiation and neglecting possible z dependence of the screening scale μ of the normalized distribution $v^2(\mathbf{q})$, we can write more explicitly at impact parameter $\mathbf{b}$

$$\frac{dN_{coh}^{VGB}}{d\eta d^2\mathbf{k}} = \frac{C_R\alpha_s}{\pi^2} \sum_{n=1}^{\infty} \left[\prod_{i=1}^{n} \int d\Delta z_i \ \sigma_{el}(z_i)\rho(z_i,\mathbf{b})\right] \left[\prod_{j=1}^{n} \int d^2\mathbf{q}_j \left(\frac{1}{\sigma_{el}}\frac{d\sigma_{el}}{d^2\mathbf{q}_j} - \delta^2(\mathbf{q}_j)\right)\right] \times \left(\frac{\mathbf{k} - \mathbf{q}_2 - \cdots - \mathbf{q}_n}{(\mathbf{k} - \mathbf{q}_2 - \cdots - \mathbf{q}_n)^2} - \frac{\mathbf{k} - \mathbf{q}_1 - \cdots - \mathbf{q}_n}{(\mathbf{k} - \mathbf{q}_1 - \cdots - \mathbf{q}_n)^2}\right) \cdot \left[\left(\frac{\mathbf{k} - \mathbf{q}_2 - \cdots - \mathbf{q}_n}{(\mathbf{k} - \mathbf{q}_2 - \cdots - \mathbf{q}_n)^2} - \frac{\mathbf{k} - \mathbf{q}_1 - \cdots - \mathbf{q}_n}{(\mathbf{k} - \mathbf{q}_1 - \cdots - \mathbf{q}_n)^2}\right) + 2\sum_{i=2}^{n} \left(\frac{\mathbf{k} - \mathbf{q}_{i+1} - \cdots - \mathbf{q}_n}{(\mathbf{k} - \mathbf{q}_{i+1} - \cdots - \mathbf{q}_n)^2} - \frac{\mathbf{k} - \mathbf{q}_i - \cdots - \mathbf{q}_n}{(\mathbf{k} - \mathbf{q}_i - \cdots - \mathbf{q}_n)^2}\right)\right] . \quad (18)$$

In order extract the the physical interpretation of the above complete but unwieldy expression, we derive in the

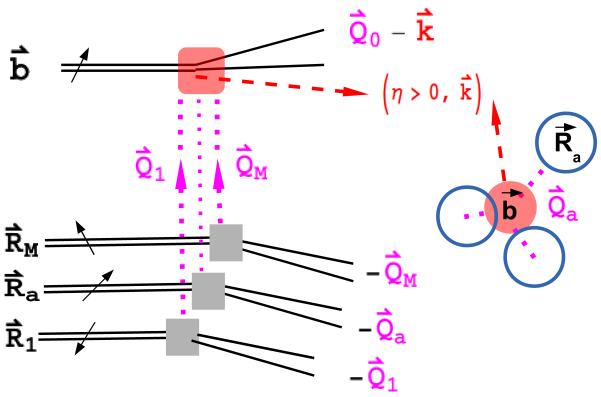

FIG. 5: (Color online) Schematic diagram corresponding to coherent bremsstrahlung from the projectile dipole from Eqs. (19,20). At opacity order n the azimuthal distribution is enhanced for transverse momenta $\mathbf{k}$ near the total accumulated momentum transfer $\mathbf{Q}_0 \equiv \mathbf{Q}_{1n} = \sum_a \mathbf{Q}_a$ where $a = 1, \cdots, M$ groups of recoiling target dipoles.

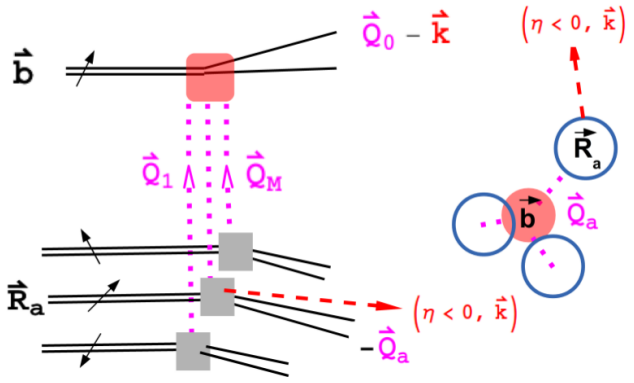

FIG. 6: (Color online) Schematic diagram corresponding to partial coherent gluon bremsstrahlung from Eqs. (23). At opacity order n the azimuthal distribution is enhanced in transverse momenta $\mathbf{k}$ near the recoil momentum transfers $-\mathbf{Q}_a$ where $a = 1, \cdots, M$ labels incoherent target groups of color dipoles fragmenting toward the negative rapidity region.

Appendix A the linked cluster theorem version of Eq. 18 to be

$$dN^{VGB}_{coh}(\mathbf{k}) = \sum_{n=1}^{\infty} \int d^2\mathbf{Q}\; P_n^{el}(\mathbf{Q})\; dN^{GB}(\mathbf{k}, \mathbf{Q}) \quad , \qquad (19)$$

where $P_n^{el}(\mathbf{Q})$ is the probability density that after n elastic scatterings the cumulative total momentum transfer is $\mathbf{Q}$,

$$P_n^{el}(\mathbf{Q}) \;=\; \exp[-\chi]\frac{\chi^n}{n!}\int \left\{\prod_{j=1}^{n}\frac{d^2\mathbf{q}_j}{\sigma_{el}}\frac{d\sigma_{el}}{d^2\mathbf{q}_j}\right\} \times\delta^2(\mathbf{Q} - (\mathbf{q}_1 + \cdots + \mathbf{q}_n)) \quad , (20)$$

that is independent of the azimuthal direction ψ of $\mathbf{Q}$ by rotation invariance. This distribution also arose naturally in the reaction operator derivation of the link cluster theorem for multiple elastic scattering in Ref. [39].

Eq. (19) is clearly the intuitive factorization limit where at each order only the total accumulated momentum transfer, $\mathbf{Q}$, controls the azimuthal and momentum transfer dependence of the bremsstrahlung distribution.

By rotation invariance $dN^{GB}(\mathbf{k}, \mathbf{Q}) = dN^{GB}(k, Q, \phi - \psi)$ can only depend on the k and Q azimuthal angles through their difference. After integrating over ψ, the azimuthal angle of $\mathbf{Q}$, then of course dN^{VGA} cannot depend on the azimuthal angle ϕ of $\mathbf{k}$. Therefore, it is obvious that at the single inclusive level all $v_n = 0$ vanish for $n > 0$. To observe the intrinsic fluctuating azimuthal asymmetries event-by-event we turn to two particle correlations to extract non-vanishing second moments like $\langle\cos(n(\phi_1 - \phi_2))\rangle$. First we discuss the bremsstrahlung contribution from recoil target participants.

IV. BREMSSTRAHLUNG FROM RECOILING TARGET PARTICIPANTS

Incoherent groups of transversely overlapping recoiling target dipoles radiate gluon bremsstrahlung dominantly into the negative rapidity $\eta < 0$ hemisphere, as illustrated in Fig. 6. In a given event when a projectile nucleon penetrates through a target nucleus A at impact parameter $\mathbf{b}$, the projectile nucleon moving with positive rapidity $Y_P > 0$ is approximated as in Ref. [35] by a color dipole with a separation $\mathbf{d}_0 = \hat{n}_0/\mu_0$. The A target nucleons moving toward negative rapidities, $Y_T < 0$, are however distributed with transverse coordinates $\mathbf{R}_i$, according to a Glauber nuclear profile distribution $T_A(\mathbf{R}_i) = \int dz \rho_A(z, \mathbf{R}_i)$ over a large area $\pi A^{2/3}$ fm^2 scale. Each target nucleon dipole is assume to have a separation $\mathbf{d}_i = \hat{n}_i/\mu_i$. Projectile target dipole-dipole interactions with low transverse momentum transfer $\mathbf{q}_i < \mu_i$ are suppressed by dipole form factors approximated by $q_i^2/(q_i^2 + \mu_i^2)$. Therefore, the projectile interacts dominantly with only nearby target dipoles in the transverse plane with $(\mathbf{R}_i - \mathbf{b})^2 \lesssim \pi\alpha^2(d_0 + d_i)^2/4 \sim \sigma_{in}$. This leads to a fluctuating number n of target participants with probability $P_n = e^{-\chi}\chi^n/n!$ that follows also from the GLV opacity expansion [37, 39, 42].

For a given target participant number, n, the target dipoles naturally cluster near the projectile impact parameter $\mathbf{b}$ as illustrated in Figs. (5,6). In a specific event, there are in general $1 \leq M \leq n$ overlapping clusters that radiate coherently toward the negative rapidity $\eta < 0$ hemisphere as illustrated in Fig.(6). The distribution of the number M of recoiling coherent groups depends on $n, \mathbf{k}$, and the momentum exchanges $\mathbf{q}_i$ with the projectile

that build up to the total exchange to the projectile

$$\mathbf{Q}_P = \sum_{a=1}^{M} \mathbf{Q}_a = \sum_{a=1}^{M} (\sum_{i\in I_a} \mathbf{q}_i) \ , \tag{21}$$

where I_a is a particular subset of the n indices $i \in [1,n] = \sum_a I_a$ that the emitted gluon with transverse wavenumber k (and generally $\eta < 0$) cannot resolve, and $\mathbf{Q}_a = \sum_{i\in I_a} \mathbf{q}_i$ is the contribution from group I_a to the total momentum transfer to the projectile.

A simple percolation model for identifying clusters of coherently recoiling target groups of dipoles is to require that all members in a cluster have separation $\mathbf{R}_{ij} = \mathbf{R}_i - \mathbf{R}_j$ in the transverse plane in modulus less than the produced gluon transverse momentum resolution scale, i.e.

$$R_{ij} \lesssim d(k) = \frac{c}{k} \ , \tag{22}$$

where $c \sim 1$ is of order unity. If $i \in I_a$ and $j \in I_a$ as well as $j \in I_b$, then j is added to I_a if its $\langle d_{ij}\rangle_{i\in I_a} < \langle d_{ij}\rangle_{i\in I_b}$. The M clusters are percolation groups in the above sense. Of course many other variants of transverse clustering algorithms exist. For our purpose of illustrating analytically dynamical sources v_n in p+A compared to peripheral $A+A$ it suffices to study the dependence of v_n on the number of independent recoil antennas M with $< n >= N$ fixed by Glauber participant geometry. In future applications via Monte Carlo generators such as HIJING [29] the sensitivity of results to more realistic multi beam jet geometric fluctuations can be studied. Note that independent target participant beam jet clusters are cylindrical cuts into the target frame near the impact parameter $\mathbf{b}$ with diameters $\sim 1/k$. We expect typically $M \sim 2-4$ independent recoil clusters even for the most central $p+A$ collisions, as illustrated in Figs. (5,6). This picture is similar to the CGC model picture except that no classical longitudinal fields are assumed in our entirely perturbative QCD dynamical bremsstrahlung approach here.

In a given event, recoil bremsstrahlung contribution to the single inclusive gluon distribution from M coherently acting but transversely resolvable target antenna clusters is given by

$$dN_T^{M,N}(\eta,\mathbf{k};\{\mathbf{q}_j\}) \equiv \sum_{a=1}^{M} dN^{GB}(\mathbf{k},-\mathbf{Q}_a)P_a(\eta) \ , \tag{23}$$

where $P_a(\eta)$ specifies different rapidity profile functions for each cluster required to produce the characteristic BGK [30] boost non-invariant triangular enhancement of the rapidity density, $(dN_{pA}/d\eta)/(dN_{pp}/d\eta)$, growing toward the value $< n >= N$ near the target rapidity Y_T and dropping toward unity near the projectile rapidity Y_p.

In the special doubly coherent projectile and target limit with $M = 1$, $dN_T^{1,N}$ reduces to

$$dN_T^{1,N}(\eta,\mathbf{k};\{\mathbf{q}_i\}_n) \equiv dN^{GB}(\mathbf{k},\ -\mathbf{Q}_P)P_T(\eta) \ , \tag{24}$$

with $P_T(\eta) = \sum_a P_a(\eta)$. Note that in the high energy small $x^- \propto \exp[Y_T - \eta]$ gluon saturation dynamics correlates $\mathbf{Q}_P$ with rapidity η instead of the simple factorization assumed in Eq. (24). In our simple perturbative dipole picture this correlation can be implemented parametrically by taking $\mu_i(\eta) \propto Q_s(\eta, A)$ [23, 46, 47].

The fully coherent projectile bremsstrahlung contribution is

$$dN_P^{M,N}(\eta,\mathbf{k};\{\mathbf{q}_i\}) \equiv dN^{GB}(\mathbf{k},\ +\mathbf{Q}_P)P_0(\eta). \tag{25}$$

For $p+p$ scattering with $M = N = 1$, the sum reduces in the CM to

$$dN_{pp} = dN^{GB}(\mathbf{k},\ +\mathbf{Q}_P)P_P(\eta)+dN^{GB}(\mathbf{k},\ -\mathbf{Q}_P)P_P(-\eta) \ , \tag{26}$$

which is symmetric with respect to changing the sign of the total momentum transfer, $\mathbf{Q}_P$, as well as to reflecting η.

In the more general partially coherent target case with $1 < M \leq N$ independent clusters of dipole antennas, the total single inclusive radiation distribution in mode $(\mathbf{k}_1,\eta_1)$ is

$$\begin{aligned} dN^{M,N} &= dN_P^N(\eta,\mathbf{k}_1;\mathbf{Q}_P) + dN_T^{M,N}(\eta,\mathbf{k}_1;\{\mathbf{Q}_a\}) \\ &= \sum_{a=0}^{M} \frac{B_{1a}}{(\mathbf{k}_1+\mathbf{Q}_a)^2+\mu_a^2} \ , \end{aligned} \tag{27}$$

where we defined $\mathbf{Q}_0 \equiv -\mathbf{Q}_P = -\sum_a \mathbf{Q}_a$ to be able to include the projectile contribution into the summation over target clusters. The numerator factor B_{ia} is defined using Eqs. (5,6) to be

$$B_{ia} \equiv F_{k_i,Q_a}\ P_a(\eta_i) \ . \tag{28}$$

For a fixed set of $\mathbf{Q}_a = (Q_a,\psi_a)$ of independent recoil momenta, the single gluon inclusive azimuthal Fourier moments $\langle\cos(n\phi)\rangle$ are given by linear combinations of $v_n^{GB}(k_1,Q_a)\cos(n\psi_a)$ from Eqs. (7)-(12). However, since all the terms in the sum contribute with one of $M+1$ $\cos(n\psi_a)$ factors, averaging over rotations $\psi_a \to \psi_a + \theta$ again causes all ensemble averaged $< v_n >= 0$ to vanish for $n \geq 1$. In order to extract information about the relative *fluctuating* v_n, we therefore turn to two gluon correlations in the next section.

V. MULTI GLUON CUMULANT AZIMUTHAL HARMONICS, $v_n\{2\ell\}$, FROM COLOR SCINTILLATION ANTENNA (CSA) ARRAYS

Multiple bremsstrahlung gluons are radiated over long ranges ("ridges") in $Y_T < \eta_i < Y_P$ from multiple kinematically and transverse space correlated beam jets that form "Color Scintillation Antenna" (CSA) arrays that fluctuate from event to event. Depending on the transverse space geometry, $\mathbf{R}_a$ and the transverse momentum transfers , $\mathbf{Q}_a$, and their distributions, the

CSA bremsstrahlung leads to fluctuating patterns of azimuthal correlations among the radiated gluons. Gluon bremsstrahlung from a single beam jet color dipole antenna builds up a "near side" correlations. Kinematic recoil momentum correlated N participant target and projectile antennas, however, also naturally radiate with $k^2 \sim N\mu^2$ in complex fluctuating azimuthal harmonic bremsstrahlung patterns. At much higher transverse momenta $k^2 \gg M\mu^2$, collinear factorized back-to-back hard jet production dominates over multiple beam jets bremsstrahlung and leads to very strong away side $n = 1$ correlations that must be subtracted in order to reveal the moderate $k^2 \lesssim M\mu^2$ correlations that we compute here. We also assume that we can neglect a possibly large in magnitude transverse isotropic nonperturbative bulk background through appropriate experimental mixed event subtraction schemes.

Assuming that M antenna clusters out of the $N = N_T^{part}(\mathbf{b})$ target participants radiate independently - i.e., assuming that each cluster in the CSA array produces approximately a semi-classical coherent state of gluon radiation with random phase with respect to other clusters (see analogous partially coherent pion interferomentry formalism in Ref.[51]) - the even number 2ℓ inclusive gluons distribution factorizes as

$$dN_{2\ell}^{M}(\eta_1, \mathbf{k}_1, \cdots, \eta_{2\ell}\mathbf{k}_{2\ell}) \;=\; \prod_{i=1}^{2\ell}\left(\sum_{a_i=0}^{M}\frac{B_{k_i a_i}}{A_{k_i a_i} - \cos(\phi_i + \psi_{a_i})}\right) \;\;, \tag{29}$$

where B_{ia} is defined in Eq. (28) and again the summation range includes the projectile $a = 0$ contribution with $\mathbf{Q}_0 \equiv -\mathbf{Q}_P$. We emphasize that the total gluon inclusive has in addition to $dN_{2\ell}^{M}$ an isotropic $dN_{2\ell}^{non.pert.}$ and a highly away side correlated $dN_{2\ell}^{dijet}$ components that we assume can be subtracted away. Implicitly we also assume here the greatly simplified "local parton hadron" duality hadronization prescription as in CGC models. Of course, in CGC saturation models the details, especially the x, A, and $\mathbf{b}$ will differ, but it is useful to explore here the basic consequences of this simple analytic model to get a feeling of how much of the azimuthal fluctuation phenomenology may have its roots in low order Low-Nussinov/Gunion-Bertsch pQCD interference phenomena. Quenching of v_n bremsstrahlung harmonics due especially to more realistic hadronization phenomenology [29, 52, 53] in the few GeV minijet scale will also need to be investigated in the future.

Even with uncorrelated gluon number coherent state product ansatz for the multi gluon inclusive distribution above, the even number $m = 2\ell$ gluons with $(\mathbf{k}_1, \eta_1)$ to $(\mathbf{k}_m, \eta_m)$ become correlated through the CSA geometric and kinematic recoil correlations.

Consider, for example, the $M = 2$ case (see Appendix B) of two recoiling target dipole antennas that emit $\mathbf{k}_1$ preferentially near $-\mathbf{Q}_1 = (q_1, \psi_1 + \pi)$ and near $-\mathbf{Q}_2 = (q_2, \psi_2 + \pi)$, at two different recoil azimuthal angles $\psi_1 + \pi$ and $\psi_2 + \pi$, while the projectile dipole emits $\mathbf{k}_2$ preferentially near $\mathbf{Q}_P = \mathbf{Q}_1 + \mathbf{Q}_2$ at a third ϕ_P azimuthal angle. Such a three color antenna system then naturally leads to two particle triangularity $v_3\{2\} \equiv \langle\cos(3(\phi_1 - \phi_2)) \neq 0$ due to dynamical correlations between $\mathbf{k}_1$ and $\mathbf{k}_2$. As we also show below in section V, special cases of Z_n symmetric antenna arrays illustrate "perfect" bremsstrahlung leading to a pure $v_{n'}\{2\} = \delta_{nn'}v_n^{Z_n}\{2\}$ two particle harmonic.

Consider in detail the prototype $M = 1$ VGB antenna case again but for 2ℓ gluon cumulant n^{th} relative harmonic moments. For a fixed $\mathbf{Q}$ impulse,

$$\begin{aligned}
f_n^{M=1}\{2\ell\} \;&\equiv\; \left\langle e^{+i\,n\left\{\sum_{i=1}^{\ell}\phi_i\right\}} e^{-i\,n\left\{\sum_{j=\ell+1}^{2\ell}\phi_j\right\}}\right\rangle \; f_0^{M=1}\{2\ell\} \\
&=\; \prod_{i=1}^{\ell}\left(\int\frac{d\phi_i}{2\pi}\frac{B_{k_iQ}\; e^{+in\phi_i}}{A_{k_iQ} - \cos(\phi_i + \psi_Q)}\right)\prod_{j=\ell+1}^{2\ell}\left(\int\frac{d\phi_j}{2\pi}\frac{B_{k_jQ}\; e^{-in\phi_j}}{A_{k_jQ} - \cos(\phi_j + \psi_Q)}\right) \\
&=\; \prod_{i=1}^{\ell}\left(e^{in\psi_Q}\,(z_{k_iQ})^n\;\, f_{0,k_i,Q}\right)\prod_{j=\ell+1}^{2\ell}\left(e^{-in\psi_Q}\,\left(z_{k_jQ}\right)^n\;\, f_{0,k_j,Q}\right) \\
&=\; f_0^{M=1}\{2\ell\}\prod_{i=1}^{2\ell}\left(v_1^{GB}(k_i, Q)\right)^n \;\;.
\end{aligned} \tag{30}$$

Note that by construction even gluon number $f_n^M\{2\ell\}$ are $SO(2)$ rotation invariant about the beam axis and thus independent of the random orientation, ψ_Q, of the reaction plane defined by the transverse momentum transfer $\mathbf{Q}$. Of course odd gluon number cumulants vanish after averaging over the reaction plane.

Here $z_{k_iQ} = A_{k_iQ} - \sqrt{A_{k_iQ}^2 - 1}$ are the poles inside the unit circle that contribute to the nth harmonics. For odd number of gluons all harmonics vanish but for even numbers all harmonics both even and odd are generated already by one $M = 1$ color GB bremsstrahlung antenna. For $M = 2$, two recoiling GB antennas, $\mathbf{Q}$ and $-\mathbf{Q}$ all odd $n = 1, 3, \cdots$ moments vanish by symmetry. An M odd number of antennas are needed to generate odd n harmonics through even number of gluon correlators.

In the "mean recoil" approximation $Q \approx \bar{Q}$, we see that a single GB antenna satisfies the generalized power scaling law in case that subsets of the 2ℓ gluons have identical momenta. Suppose there are $1 \leq L \leq 2\ell$ distinct momenta K_r with $r = 1, \cdots, L$ such m_r of the 2ℓ gluons have momenta equal to a particular value K_r such that $\sum_{r=1}^{L} m_r = 2\ell$. In this case

$$v_n^{M=1}\{2\ell\}(k_1, \cdots, k_{2\ell}; \bar{Q}) \approx \prod_{r=1}^{L} (v_n^{GB}(K_r, \bar{Q}))^{m_r} = \prod_{r=1}^{L} (v_1^{GB}(K_r, \bar{Q}))^{nm_r} \quad . \tag{31}$$

This approximate mean recoil factorization and remarkable power scaling of coherent state semi-classical bremsstrahlung wave harmonics leads to an apparent "perfect fluid collective flow" interpretation.

Higher order cumulant harmonic correlations were proposed [55**?** –57] to help remove "non-flow" sources of correlations such as momentum conservation, back to back dijet, and Bose statistics effects and isolate true collective bulk fluid flow azimuthal asymmetries. The 2ℓ-particle cumulant suppresses "non-flow" contribution by eliminating the correlations which act between fewer than 2ℓ particles (see. e.g., fig.9 of [57]). The first few cumulants for $2\ell = 2, 4, 6$ (notation from from Ref. [56, 57]) are

$$\begin{aligned}
(v_n\{2\})^2 &\equiv \left\langle e^{in(\phi_1 - \phi_2)} \right\rangle \equiv \langle |v_2|^2 \rangle \\
(v_n\{4\})^4 &\equiv \left\langle -e^{in(\phi_1 + \phi_2 - \phi_3 - \phi_4)} \right\rangle + 2 \left\langle e^{in(\phi_1 - \phi_3)} \right\rangle \left\langle e^{in(\phi_2 - \phi_4)} \right\rangle = 2\langle |v_2|^2 \rangle^2 - \langle |v_n|^4 \rangle \\
(v_n\{6\})^6 &\equiv \left\langle e^{in(\phi_1 + \phi_2 + \phi_3 - \phi_4 - \phi_5 - \phi_6)} \right\rangle - 9 \left\langle |v_2|^2 \right\rangle \left\langle |v_n|^4 \right\rangle + 12 \left\langle |v_2|^2 \right\rangle^3)/4 \quad .
\end{aligned} \tag{32}$$

The observed [57] near equality of $v_n\{2\ell\}$ for $\ell = 2, 3, 4$ in $Pb + Pb$ at LHC has been interpreted as strong evidence for perfect fluid flow. The similarity of "elliptic flow" $v_2\{4\}(p_T)$ in p+Pb and Pb+Pb observed by ATLAS[4] and also for "triangular flow" $v_3\{4\}(p_T)$ by CMS[2] has been interpreted as evidence for perfect fluidity also on sub-nucleon scales in p+Pb.

However, we show that color bremsstrahlung exhibits the same scaling of cumulants in the mean recoil approximation from a single antenna. In the case that all 2ℓ momenta are identical,

$$\bar{v}_n\{2\ell\} \equiv (v_m^{M=1}\{2\ell\}(k, \cdots, k; \bar{Q}))^{n/m} \tag{33}$$

which in the previous notation implies, for example, that

$$\langle |v_n|^4 \rangle = \left\langle |v_2|^2 \right\rangle^2 \tag{34}$$

$$\langle |v_6|^6 \rangle = \langle |v_2|^2 \rangle \langle |v_n|^4 \rangle = \left\langle |v_2|^2 \right\rangle^3 \tag{35}$$

and similarly for all cumulants. Therefore color bremsstrahlung obeys the *the same* azimuthal harmonic cumulant independence on the number of gluons 2ℓ used to determine the harmonic moments as does perfect fluid local equilibrium. However in our case, the "flow" effect comes purely from zero temperature pure coherent state (semi-classical) wave interference effects produced from the geometric arrangement of CSA arrays .

For the case of multiple $M > 1$ independent target cluster CSA arrays the cumulant harmonic moments depend in a more complex way on the particular geometric and recoil correlations defining the CSA. Special analytic cases for $v_2\{2\}$ considered corresponding to idealized Z_n and Gaussian CSA arrays are illustrated in the following two sections.

VI. EXAMPLE OF SPECIAL Z_N CSA ARRAY BREMSSTRAHLUNG

As see in Appendix B, from Eqs. (53) it is clear that a particularly simple special cases of color antenna arrays where $M = n - 1$ target beam jet clusters all have similar number of recoiling target partons $m_a = N/M = N/(n-1)$ and for which transfer all $n = M + 1$ projectile and target beam jets recoil with similar momentum transfers, $Q_a^2 = N/M\mu^2$, but with specially spaced azimuthal angles, $\{\psi_a\} = 2\pi a/n$.

These particular color antenna arrays that we will refer to as Z_n Color Scintillation Arrays (CSA) have a special discrete azimuthal rotation symmetry corresponding to

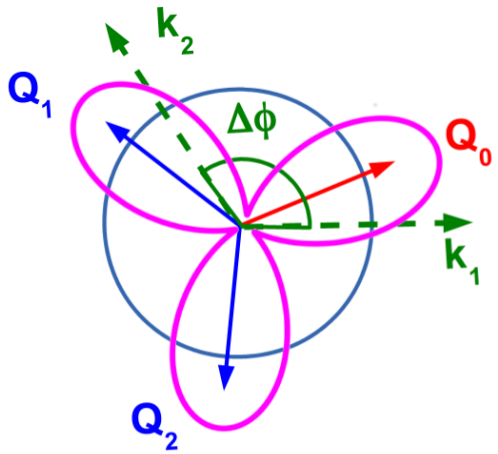

(a)

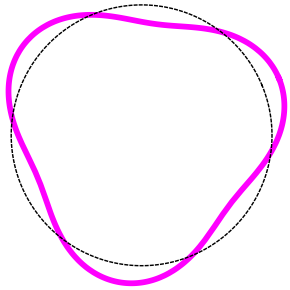

(b)

FIG. 7: (Color online) Example illustrating apparent perfect "triangular flow" using Z_3 Color Scintillation Antenna arrays with $M = 2$ target clusters recoiling off projectile with $\mathbf{Q}_0 = -\sum_{a=1}^{M} \mathbf{Q}_a$. All Q_a are assumed to have same magnitude but spaced by $2\pi/3$ in azimuthal angle. Z_n CSA radiate "perfect" factorized two particle n^{th} harmonics $v_n\{2\}(k_1, k_2) = \delta_{n,3}\ v_3^{GB}(k_1, Q_0)v_3^{GB}(k_2, Q_0)$. Part (a) shows extreme case $v_3 = 0.45$ while (b) is for more realistic $v_3 = 0.07$. The isotropic soft non perturbative background is assumed to be subtracted out.

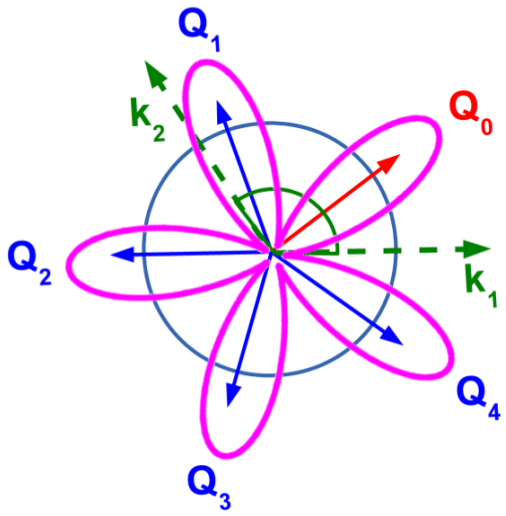

(a)

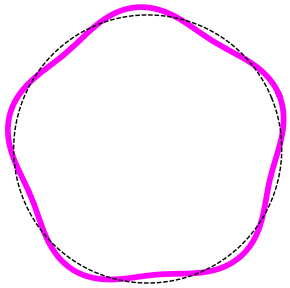

(b)

FIG. 8: (Color online) As in Fig. 7 but for a Z_5 CSA producing apparent perfect pentatonic flow $v_n\{2\}(k_1, k_2) = \delta_{n,5}\ v_5^{GB}(k_1, Q_0)v_5^{GB}(k_2, Q_0)$. Part (a) show extreme $v_5 = 0.45$ while part (b) shows more realistic $v_5 = 0.03$.

the finite group of n roots of unity,

$$Z_n = \left\{ z_{a,n} = e^{i2\pi a/n} | a = 0, \cdots, n-1; \sum_{a=0}^{n-1} z_{a,n} = 0 \right\} \ . \tag{36}$$

For these Z_n CSA geometries of projectile and target color dipole antennas the double sum over a and b is trivial because

$$\cos(n(\psi_a - \psi_b)) = \cos(2\pi(a-b)) = 1 \ , \tag{37}$$

and thus all $(M+1)^2 = n^2$ terms are identical. Note that Eq.(37) is invariant to global $SO(2)$ simultaneous rotations of all antennas.

What is remarkable about Z_{M+1} symmetric CSA is that due to the orthogonality properties of the z_{an} phases,

$$\sum_{a=1}^{n-1} z_{a,n}^k = n\delta_{k,n} \tag{38}$$

$$\sum_{a=1}^{n-1} (z_{a,n})^k (z_{a,n}^*)^{k'} = n\delta_{k,k'} \ , \tag{39}$$

all harmonics except $n = M+1$ vanish! The Z_n CSA thus scintillate with "perfect" n-harmonic azimuthal correlations. For Z_n CSA the two particle relative Fourier moments $v_n\{2\}$ simply factor into a product of single particle moments $v_n^{GB}(k_i, Q_0, 0)$ because the n complex $Q_a = Q_0 z_{a,n}$ form a regular polygon with equal radii as illustrated for an $n = 5$ "star fish" antenna array in Fig. (7) that generate a perfect $\cos(5(\phi_1 - \phi_2))$ two particle azimuthal correlation.

For roots of unity CSA color antenna geometries all $M+1$ antennas receive the same $Q_a^2 = Q_0^2 = N/(n-1)\mu^2$ momentum transfer and produce the same single particle $v_{M+1}^{GB}(k, Q_0, 0)$ harmonics. Since the two particle

harmonics vanish except for $n = M + 1$,

$$v_n^{M,N}\{2\}(k_1,k_2) \xrightarrow{Z_n} \delta_{n,M+1} v_{M+1}^{GB}(k_1,Q_0) v_{M+1}^{GB}(k_2,Q_0)$$
$$\frac{v_n^{M,N}\{2\}(k_1,k_2)}{v_{M+1}^{GB}(k_2,Q_0)} \xrightarrow{Z_n} \delta_{n,M+1}\,(v_1^{GB}(k_1,Q_0))^{M+1}\ , \quad (40)$$

and for $n = M+1$, $v_{M+1}^{M,N}\{2\}(k_1,k_2)$ is reduced to simply the product of single GB CSA moments at k_1 and k_2.

Examples of Z_n radiation patterns for $n = 3, 5$ for extreme high $v_n = 0.45$ in parts (a) and more realistic $v_3 = 0.7$ and $v_5 = 0.03$ from Fig. (1) are shown in Figs. (7,8).

VII. GAUSSIAN COLOR SCINTILLATION ANTENNA ARRAYS

Another simple limit is when the recoil azimuthal angles ψ_a are in random $[0, 2\pi]$ and the $\mathbf{Q}_a$ are distributed with a Gaussian of same width squared $\langle Q_a^2\rangle = Q_T^2 = (N/M)\mu^2$ for $a \in [1, \cdots, M]$. In this antenna array, the projectile $\mathbf{Q}_0$ is also Gaussian distributed with zero mean but with an enhanced second moment,

$$\langle Q_0^2\rangle = MQ_T^2 = N\mu^2\ . \quad (41)$$

Unlike for perfect n^{th} harmonic antenna arrays with Eq. (37), in the random Gaussian distributed case

$$\cos(n(\psi_a - \psi_b)) = \delta_{a,b}\ , \quad (42)$$

and so only the $a = b$ diagonal terms contribute. All $a \geq 1$ target terms are identical and only the projectile contribution is enhanced due to $\langle Q_0^2\rangle/Q_T^2 = M$ random walk exchanges from each cluster. In this case, Eq.(53) reduces to

$$f_n^{N,M}(k_1,k_2) \overset{Gauss}{\to} \int d^2\mathbf{Q}\left\{\frac{\exp[-\mathbf{Q}^2/(2N\mu^2)]}{2\pi N\mu^2} + M\frac{\exp[-\mathbf{Q}^2/(2(N/M)\mu^2)]}{2\pi(N/M)\mu^2}\right\}\{B_{1Q}B_{2Q}\ f_{0,1,Q}\ f_{0,2,Q} \times v_n^{GB}(k_1,Q)\ v_n^{GB}(k_2,Q)\}\ , \quad (43)$$

$$f_n^{N,M}(k,k) \overset{Gauss}{\to} \int d^2\mathbf{Q}\left\{\frac{\exp[-Q^2/(2N\mu^2)]}{2\pi N\mu^2} + M\frac{\exp[-Q^2/(2(N/M)\mu^2)]}{2\pi(N/M)\mu^2}\right\}\{B_{kQ}f_{0,k,Q}v_n^{GB}(k,Q)\}^2\ . \quad (44)$$

We have suppressed target and projectile kinematic rapidity factors.

To get a feeling for the magnitude of the two particle azimuthal moments we can approximate Q in the integrand outside the Gaussian weights by its rms $\Delta Q = \sqrt{\langle Q^2\rangle}$ and perform the normalized integral over the Gaussians to estimate

$$\sqrt{f_n^{N,M}(k,k)} \approx \left(\frac{C_R\alpha_s\mu^2}{\pi^2k^2}\right)\left\{\frac{1}{(N+1)\mu^2}\frac{(v_1^{GB}(k,\sqrt{N}\mu))^n}{((k^2+(N+1)\mu^2)^2-4Nk^2\mu^2)^{1/2}} + \frac{M}{(N/M+1)\mu^2}\frac{(v_1^{GB}(k,\sqrt{N/M}\mu))^n}{((k^2+(N/M+1)\mu^2)^2-4(N/M)k^2\mu^2)^{1/2}}\right\}\ . \quad (45)$$

The rapidity dependence corresponding to the BGK[30] triangular rapidity enhancement $N(Y_P-\eta)/(Y_P-Y_T)$ of the single inclusive multiplicity toward the target fragmentation region is suppressed above to simplify the result. In addition we emphasize that the mostly non-perturbative low k background is ignored in our simplified consideration here. Full account for that background will require implementation of the above non-isotropic soft bremsstrahlung in an event generator such as HIJING.

A qualitative BGK[30] rapidity dependence for target cluster number $M(\eta)$ that ignores the c/k resolution scale considerations discussed in Eq. (22) can be estimated by identifying $N = \chi = \int dz\rho_A(z,\mathbf{b})$ with the opacity as a function of b and taking

$$M_{BGK}(\eta) \sim \chi(Y_P-\eta)/(Y_P-Y_T)(1-e^{Y_T-\eta})^{n_f}\ . \quad (46)$$

The main feature expected from BGK[30] rapidity dependence of the target cluster bremsstrahlung is that the $v_n\{2\ell\}$ cumulant harmonics depend on the η_i in a characteristic way that reflects underlying triangular BGK $p+A$ inclusive boost non-invariant inclusive rapidity distribution. There is also a rather nontrivial combined (η_i, k_i) variation of the moments due to the peaking of the $v_n^{GB}(k,Q)$ near $k^2 = Q^2$ and the fact that target cluster rapidity dependent recoil $k^2 = (N/M(\eta))\mu^2$ varies with η while the fully coherent Cronin enhanced $k^2 \sim N\mu^2$ projectile peak increases with the opacity $N \sim L/\lambda = \chi$. Detailed numerical studies of combined (η, k) dependence of azimuthal color bremsstrahlung will be explore elsewhere.

VIII. HIJING MONTE CARLO COLOR SCINTILLATING BEAM JETS

To get a realistic estimate for the magnitudes and systematics of pQCD VGB induced harmonics in realistic $p+p, p+A, A+A$ collisions, we have to embed the anisotropic recoil bremsstrahlung gluons into phenomenological Lund strings Schwinger hadronization scheme that has been tuned to reproduce low p_T ϕ *averaged* inclusive hadronic observables in $e^+ + e^-$, $e+p$, $p+p$, $p+A$, as well as $A+A$. HIJING Monte Carlo event generator is one such model based on the LUND [52] string model and PYTHIA and JETSET [53] Monte Carlo models.

Simple local parton-hadron duality prescription as used in CGC cannot be expected to predict quantitative hadron mass dependent moderate $p_T < 2$ GeV anisotropy moments over three decades of $\sqrt{s}$. The advantage of Monte Carlo event generators built on multi-decade phenomenological analysis is that they summarize the world data by taking into account the particle data book, quantum number, and energy momentum conservation and numerous Standard Model dynamical details. Of course, they do not proport to cover all possible phenomena.

A key feature missing in HIJING and most other event generators for $A+B$ collisions so far are basic pQCD azimuthal anisotropies at the moderate $p_T < 2$ GeV scale that are so clearly predicted by GB and generalized VGB bremsstrahlung models. What has been included in most event generators are strong jet anisotropies due to collinear factorized pQCD mini and hard jet production above a scale $p_T > p_0 \sim 2$ GeV. As currently implemented, HIJING only take into softer scale $k < p_0$ gluons as random transverse string "wiggles" using ARIADNE [54] Lund model scheme, but it neglects entirely the basic pQCD recoil correlations so explicitly seen in the GB and VGB bremsstrahlung expressions. An open question is the magnitude of the anisotropies that will arise when the ARIANDE part of the JETSET code is replaced by VGB anisotropic bremsstrahlung as derived here. We intend to address this numerically intensive work as a future application of the formulas derived in this paper.

IX. CONCLUSIONS

In summary, we applied the GLV reaction operator approach to the Vitev-Gunion-Bertsch (VGB) boundary conditions to compute the all-order in nuclear opacity non-abelian gluon bremsstrahlung of event-by-event fluctuating beam jets in nuclear collisions. We obtained analytic expressions for the azimuthal Fourier cumulant moments $v_n\{2\ell\}$ as a function of the gluons kinematics $\mathbf{k}_i, \eta_i\}$ in terms of single gluon beam jet GB bremsstrahlung harmonics. These moments obey remarkably simple power law scaling similar to the ones observed recently in high energy p+A reactions at RHIC and LHC as a function of the target participant clusters geometry. Multiple clusters of projectile and target beam jets form Color Scintillation Antenna (CSA) arrays that radiate gluons with characteristic boost non-invariant trapezoidal rapidity distributions in asymmetric $B+A$ nuclear collisions. The intrinsically azimuthally anisotropic and long-range in η nature of the non-abelian bremsstrahlung leads to v_n moments that are similar to results from perfect fluid hydrodynamic models, but due entirely to non-abelian wave interference phenomena sourced by the fluctuating CSA. We presented examples of simple solvable models of target dipole clusters and showed that our analytic non-flow bremsstrahlung solutions for $v_n\{2\ell\}$ are similar to recent numerical saturation model predictions but differ by predicting a simple power-law hierarchy of both even and odd $v_n\{2\ell\}$ without invoking details of k_T factorization, though CGC saturation evolution is expected to be important for future quatitative comparisons to data. The basic CSA mechanism can be tested via its predicted systematic boost non-invariant η rapidity dependence in $B+A$

Non-abelian beam jet CSA bremsstrahlung investigated in this paper may provide a partial analytic solution to the Beam Energy Scan (BES) discovery of the near $\sqrt{s}$ independence of the azimuthal moments down to very low CM energy of ~ 10 AGeV, where large x valence quark beam jets dominate inelastic dynamics. Recoil bremsstrahlung from multiple independent CSA clusters also provides a natural pQCD qualitative explanation for the unexpected similarity of v_n in $p(D)+A$ and non-central $A+A$ at same $dN/d\eta$ multiplicity as observed at RHIC and LHC.

This PQCD based model show that the uniqueness of perfect fluid descriptions of $p+A$ and $B+A$ data cannot be taken for granted. However, a great deal of work remains to sort out the fraction of the observed $v_n\{2\ell\}$ azimuthal harmonic systematics that can be properly ascribed to final state bulk collective flow versus QCD coherent state color scintillating wave interference phenomena.

X. APPENDIX: THE LINKED CLUSTER THEOREM FOR COHERENT VGB GLUON BREMSSTRAHLUNG

To derive the link cluster theorem for the coherent limit of VGA we introduce the shorthand notation for the integrations over momentum transfers

$$\prod_{j=1}^{n}\int d(w_j-\delta_j) \equiv \int \prod_{j=1}^{n} d^2\mathbf{q}_j \left(\frac{1}{\sigma_{el}}\frac{d\sigma_{el}}{d^2\mathbf{q}_j} - \delta^2(\mathbf{q}_j)\right) , \tag{47}$$

which have the convenient properties $\int dw_j = \int d\delta_j = 1$ and $\int d(w_j - \delta_j) = 0$, that is particularly useful to be able to discard any terms in the integrand that does not depend simultaneously on all n $\mathbf{q}_j$ momenta at fixed opacity order n. Using this shorthand and $\mathbf{C}_{jn}$ notation from Eqs.16, we rewrite the right hand side of Eq. (18) as

$$\begin{aligned}
VGB &= \frac{C_R\alpha_s}{\pi^2}\sum_{n=1}^{\infty}\frac{\chi^n}{n!}\left[\prod_{j=1}^{n}\int d(w_j-\delta_j)\right] \\
&\quad \times (\mathbf{C}_{2n}-\mathbf{C}_{1n})\cdot\left[(\mathbf{C}_{2n}-\mathbf{C}_{1n}) + 2\,(\mathbf{C}_{3n}-\mathbf{C}_{2n}) + \cdots + 2\left(\mathbf{C}_{(n+1)n}-\mathbf{C}_{nn}\right)\right] \\
&= \frac{C_R\alpha_s}{\pi^2}\sum_{n=1}^{\infty}\frac{\chi^n}{n!}\left[\prod_{j=1}^{n}\int d(w_j-\delta_j)\right](\mathbf{C}_{2n}-\mathbf{C}_{1n})\cdot[(\mathbf{C}_{2n}-\mathbf{C}_{1n}) + 2\,(\mathbf{H}-\mathbf{C}_{2n}))] \\
&= \frac{C_R\alpha_s}{\pi^2}\sum_{n=1}^{\infty}\frac{\chi^n}{n!}\left[\prod_{j=1}^{n}\int d(w_j-\delta_j)\right][-(\mathbf{H}-\mathbf{C}_{2n}) + (\mathbf{H}-\mathbf{C}_{1n})]\cdot[(\mathbf{H}-\mathbf{C}_{2n}) + (\mathbf{H}-\mathbf{C}_{1n})] \\
&= \frac{C_R\alpha_s}{\pi^2}\sum_{n=1}^{\infty}\frac{\chi^n}{n!}\left[\prod_{j=1}^{n}\int d(w_j-\delta_j)\right]\left\{|\mathbf{H}-\mathbf{C}_{1n}|^2 - |\mathbf{H}-\mathbf{C}_{2n})|^2\right\} \\
&= \frac{C_R\alpha_s}{\pi^2}\sum_{n=1}^{\infty}\frac{\chi^n}{n!}\left[\prod_{j=1}^{n}\int d(w_j-\delta_j)\right]|\mathbf{H}-\mathbf{C}_{1n}|^2 \\
&= \sum_{n=1}^{\infty}\frac{\chi^n}{n!}\left[\prod_{j=1}^{n}\int d(w_j-\delta_j)\right]\left(\int d^2\mathbf{Q}\;\delta^2(\mathbf{Q}-(\mathbf{q}_1+\cdots+\mathbf{q}_n))\right)\left\{\frac{C_R\alpha_s}{\pi^2}\frac{\mathbf{Q}^2}{k^2(\mathbf{k}-\mathbf{Q})^2}\right\} .
\end{aligned} \tag{48}$$

Here, we used the notation $\mathbf{H} \equiv \mathbf{C}_{(n+1),n} \equiv \mathbf{k}/k^2$ to denote the "hard" vacuum radiation amplitude that shows up at zeroth order in opacity in the case final state induced radiation in GLV [37]. Note that in this notation convention $\mathbf{B}^n_{(n+1),n)} \equiv \mathbf{H} - \mathbf{C}_{nn}$.

Note that $\int d(w_j - \delta_j) = 0$, and therefore $j = 1$ integral of $-|\mathbf{H}-\mathbf{C}_{2n}|^2$ automatically vanishes. Note further that the $|\mathbf{H} - \mathbf{C}_{1n}|^2$ integrand depends only on $\mathbf{k}$ and the *Total* accumulated $\mathbf{Q} = \sum_{i=1}^{n}\mathbf{q}_i$ momentum transfer. Thus, the integrand is symmetric under arbitrary permutations if the indices. This is the key to obtain the linked cluster rearrangement because out of the the 2^n combinations of the w_j and minus delta functions $-\delta_i$, all combinations with the same number m of $\int dw$ and $n-m$ of $\int d\delta$ integrations give the same contribution. At fixed opacity order n the 2^n combinations of integrals reduce to sum over only n integrals of the form $n!/(m!(n-m)!)\int dw_1\cdots dw_m(-1)^{n-m}|B^m_{1m}|^2$. Therefore,

$$\frac{dN^{VGB}_{coh}}{d\eta d^2\mathbf{k}} = \sum_{n=1}^{\infty}\frac{\chi^n}{n!}\sum_{m=1}^{n}\frac{(-1)^{n-m}\,n!}{m!(n-m)!}\int d^2\mathbf{Q}\left[\int dw_1\cdots dw_m\delta^2(\mathbf{Q}-(\mathbf{q}_1+\cdots+\mathbf{q}_m))\right]\left\{\frac{C_R\alpha_s}{\pi^2}\frac{Q^2}{k^2(\mathbf{k}-\mathbf{Q})^2}\right\} . \tag{49}$$

Changing summation variables from, $\infty > n \geq 1$ and $n \leq m \geq 1$ to $\infty > \ell = n - m \geq 0$ and $\infty > m \geq 1$, the double sum $\sum_{\ell=0}^{\infty}\sum_{m=1}^{\infty}$ factorizes, and the sum over ℓ

produces a factor $\exp[-\chi]$ corresponding to the probability of no scattering. Therefore, Eq.(49) leads to link cluster theorem Eq.(19) for the multiple collision VGB generalization of Gunion-Bertsch gluon bremsstrahlung .

XI. APPENDIX B: TWO GLUON BREMSSTRAHLUNG AZIMUTHAL HARMONICS $v_n\{2\}$

For the two gluon case azimuthal harmonic correlations can be directly derived in another way by integrating over both $\phi_1 = \Phi + \Delta\phi/2$ and $\phi_2 = \Phi - \Delta\phi/2$ keeping the relative azimuthal angle $\Delta\phi = \phi_1 - \phi_2$ fixed and weighing the integrand by $\cos(n\Delta\phi)$ from

$$
\begin{aligned}
f_n^M\{2\}(k_1,k_2) \;\equiv\; & \int_{-\pi}^{\pi}\frac{d\Phi}{2\pi}\int_{-\pi}^{\pi}\frac{d\Delta\phi}{2\pi}\,\cos(n\Delta\phi)dN_2^M(k_1,\Phi+\Delta\phi/2,k_2,\Phi-\Delta\phi/2) \\
=&\sum_{a,b=0}^{M} B_{1a}B_{2b}\int_{-\pi}^{\pi}\frac{d\Delta\phi}{2\pi}\,\cos(n\Delta\phi)\int_{-\pi}^{\pi}\frac{d\Phi}{2\pi}\frac{1}{A_{1a}-\cos(\Phi+\psi_a+\Delta\phi/2)}\frac{1}{A_{2b}-\cos(\Phi+\psi_b-\Delta\phi/2)} \qquad (50)\\
=&\sum_{a,b=0}^{M} B_{1a}B_{2b}\int_{-\pi}^{\pi}\frac{d\Phi'}{2\pi}\frac{1}{A_{1a}-\cos(\Phi')}\int_{-\pi}^{\pi}\frac{d\Delta\phi}{2\pi}\frac{\cos(n\Delta\phi)}{A_{2b}-\cos((\Phi'+\psi_b-\psi_a)-\Delta\phi)} \qquad (51)\\
=&\sum_{a,b=0}^{M} B_{1a}B_{2b}\,f_{n,2,b}\int_{-\pi}^{\pi}\frac{d\Phi'}{2\pi}\frac{\cos(n(\Phi'+\psi_b-\psi_a))}{A_{1a}-\cos(\Phi')} = \sum_{a,b=0}^{M} B_{1a}B_{2b}\,f_{n,2,b}\,f_{n,1,a}\,\cos(n(\psi_b-\psi_a)) \qquad (52)\\
=&\sum_{a,b=0}^{M} B_{1a}B_{2b}\,f_{0,1,a}\,f_{0,2,b}\,(v_1^{GB}(k_1,Q_a)v_1^{GB}(k_2,Q_b))^n\,\cos(n(\psi_b-\psi_a))\;, \qquad (53)
\end{aligned}
$$

where we defined $\Phi' = \Phi+\psi_a+\Delta\phi/2$ and used periodicity of the integrand to shift the Φ' range back to $[-\pi,\pi]$ in Eq. (51), then performed the $\Delta\phi$ integral with the help of Eq. (7). We used here the shorthand notation

$$
f_{n,1,a} = \int_{-\pi}^{\pi}\frac{d\Phi}{2\pi}\,\frac{\cos(n\Phi)}{A_{1a}-\cos(\Phi)} = (v_1^{GB}(k_1,Q_a))^n f_{0,1,a}, \qquad (54)
$$

$$
f_{n,1,a} = \frac{\left(A_{k_1,Q_a}-\sqrt{A_{k_1,Q_a}^2-1}\right)^n}{\sqrt{A_{k_1,Q_a}^2-1)}} \qquad (55)
$$

$$
\lim_{\mu\to 0}\; f_{n,1,a} = \left(\frac{k_1}{Q_a}\right)^n\frac{\theta(Q_a-k_1)}{Q_a^2-k_1^2}Q_a^2\;. \qquad (56)
$$

XII. ACKNOWLEDGMENTS

MG is grateful to W. Busza, J. Harris, J. Jia, A. Poszkanzer, H.J. Ritter, N. Xu for discussion related to RHIC and LHC flow experiments, and to A. Dumitru, T. Lappi, L. McLerran, J. Noronha, H. Stoecker, G. Torieri, and R. Venugopalan for critical discussions related to hydrodynamic and QCD field theory models of A+A correlations. MG acknowledges support from the US-DOE Nuclear Science Grant No. DE-FG02-93ER40764, partial sabbatical support from LBNL under DOE No. DE-AC02-05CH11231, the Yukawa Institute for Theoretical Physics, Kyoto University, the YITP-T-13-05 on "New Frontiers in QCD" workshop support, and sabbatical support from the MTA Wigner RCP, Budapest, where this work was finalized. PL and TB acknowledge support from Hungarian OTKA grants K81161, K104260, NK106119, and NIH TET_12_CN-1-2012-0016. IV was supported in part by the US Department of Energy, Office of Science.

[1] A. Adare *et al.* [PHENIX Collaboration], Phys. Rev. Lett. **111**, 212301 (2013).
[2] S. Chatrchyan *et al.* [CMS Collaboration], Phys. Lett. B **718**, 795 (2013).
[3] B. Abelev *et al.* [ALICE Collaboration], Phys. Lett. B **719**, 29 (2013).
[4] G. Aad *et al.* [ATLAS Collaboration], Phys. Rev. Lett. **110**, 182302 (2013); Phys. Lett. B **725**, 60 (2013).
[5] J. Adams *et al.* [STAR Collaboration], Nucl. Phys. A **757**, 102 (2005) [nucl-ex/0501009].
[6] K. Adcox *et al.* [PHENIX Collaboration], Nucl. Phys. A **757**, 184 (2005) [nucl-ex/0410003].
[7] A. Adare *et al.* [PHENIX Collaboration], Phys. Rev. Lett. **105**, 062301 (2010).
[8] K. Aamodt *et al.* [ALICE Collaboration], Phys. Lett. B **708**, 249 (2012).
[9] K.Aamodt *et al.* [ALICE Collaboration], Phys. Rev. Lett. **105**, 252302 (2010).
[10] Phys. Rev. Lett. **107**, 032301 (2011).
[11] S. Chatrchyan *et al.* [CMS Collaboration], Eur. Phys. J. C **72**, 2012 (2012).
[12] G. Aad *et al.* [ATLAS Collaboration], Phys. Rev. C **86**, 014907 (2012)
[13] ATLAS collab, http://cds.cern.ch/record/1702976, Quark Matter 2014, Darmstadt, Germany, May 18, 2014, ATLAS-CONF-2014-021, fg.24.
[14] J. Jia, ibid, private communication.
[15] L. Adamczyk *et al.* [STAR Collaboration], Phys. Rev. C **88**, no. 1, 014902 (2013).
[16] P. Romatschke and U. Romatschke, Phys. Rev. Lett. **99**, 172301 (2007);
[17] M. Luzum and P. Romatschke, Phys. Rev. C **78**, 034915 (2008); Phys. Rev. Lett. **103**, 262302 (2009).
[18] B. H. Alver, C. Gombeaud, M. Luzum and J. -Y. Ollitrault, Phys. Rev. C **82**, 034913 (2010).
[19] C. Gale, S. Jeon, B. Schenke, P. Tribedy and R. Venugopalan, Phys. Rev. Lett. **110**, 012302 (2013).
[20] U. Heinz and R. Snellings, Ann. Rev. Nucl. Part. Sci. **63**, 123 (2013).
[21] P. Danielewicz and M. Gyulassy, Phys. Rev. D **31**, 53 (1985); T. Hirano and M. Gyulassy, Nucl. Phys. A **769**, 71 (2006).
[22] P. Bozek, Phys. Rev. C **85**, 014911 (2012). P. Bozek and W. Broniowski, Phys. Rev. C **88**, no. 1, 014903 (2013); arXiv:1403.6042 [nucl-th].
[23] K. Dusling and R. Venugopalan, Phys. Rev. D **87** 094034 (2013).
[24] D. Teaney, J. Lauret and E. V. Shuryak, Phys. Rev. Lett. **86**, 4783 (2001) [nucl-th/0011058].
[25] G. Agakichiev *et al.* [CERES/NA45 Collaboration], Phys. Rev. Lett. **92**, 032301 (2004); D. Adamova *et al.* [CERES Collaboration], Nucl. Phys. A **894**, 41 (2012)
[26] G. Basar and D. Teaney, arXiv:1312.6770 [nucl-th].
[27] J. Auvinen and H. Petersen, Phys. Rev. C **88**, 064908 (2013); arXiv:1310.7751 [nucl-th].
[28] Y. . B. Ivanov, arXiv:1401.2265 [nucl-th].
[29] X. -N. Wang and M. Gyulassy, Phys. Rev. D **44** (1991) 3501.
[30] S. J. Brodsky, J. F. Gunion and J. H. Kuhn, Phys. Rev. Lett. **39**, 1120 (1977).
[31] A. Adil and M. Gyulassy, Phys. Rev. C **72**, 034907 (2005).
[32] R. Debbe for [ATLAS Collab], Quark Matter 2014, Darmstadt, Germany, May 19-24, 2014, ATLAS-CONF-2014-021,
[33] M. Gyulassy and L. McLerran, Nucl. Phys. A **750**, 30 (2005) [nucl-th/0405013].
[34] W. Busza, Acta Phys. Polon. B **35**, 2873 (2004) [nucl-ex/0410035].
[35] J. F. Gunion and G. Bertsch, Phys. Rev. D **25**, 746 (1982).
[36] S. J. Brodsky and J. F. Gunion, Phys. Rev. D **17**, 848 (1978).
[37] M. Gyulassy, P. Levai and I. Vitev, Nucl. Phys. B **594**, 371 (2001); Phys. Rev. Lett. **85**, 5535 (2000).
[38] M. Gyulassy, I. Vitev, X. N. Wang and B. W. Zhang, nucl-th/0302077, in R. C. Hwa and X. N. Wang editors, *Quark-Gluon Plasma III*, 123 (2004); I. Vitev, J. Phys. G **30**, S791 (2004)
[39] M. Gyulassy, P. Levai and I. Vitev, Phys. Rev. D **66**, 014005 (2002); A. Adil, M. Gyulassy, W. A. Horowitz and S. Wicks, Phys. Rev. C **75**, 044906 (2007); A. Adil and I. Vitev, Phys. Lett. B **649**, 139 (2007).
[40] M. Djordjevic and M. Gyulassy, Nucl. Phys. A **733**, 265 (2004).
[41] S. Wicks, W. Horowitz, M. Djordjevic and M. Gyulassy, Nucl. Phys. A **784**, 426 (2007) [nucl-th/0512076].
[42] I. Vitev, Phys. Rev. C **75**, 064906 (2007) [hep-ph/0703002].
[43] J. -w. Qiu and I. Vitev, Phys. Lett. B **632**, 507 (2006) [hep-ph/0405068].
[44] R. B. Neufeld, I. Vitev and B. -W. Zhang, Phys. Lett. B **704**, 590 (2011).
[45] Z. -B. Kang, I. Vitev and H. Xing, Phys. Lett. B **718**, 482 (2012).
[46] D. Kharzeev, E. Levin and L. McLerran, Nucl. Phys. A **748**, 627 (2005) [hep-ph/0403271].
[47] T. Lappi and L. McLerran, Nucl. Phys. A **772**, 200 (2006); T. Lappi, Phys. Lett. B **643**, 11 (2006).
[48] J. Noronha and A. Dumitru, Phys. Rev. D **89**, 094008 (2014).
[49] G. Ovanesyan and I. Vitev, JHEP **1106**, 080 (2011).
[50] K. Dusling and R. Venugopalan, Phys. Rev. D **87**, no. 5, 051502 (2013).
[51] M. Gyulassy, S. K. Kauffmann and L. W. Wilson, Phys. Rev. C **20**, 2267 (1979).
[52] B. Andersson, G. Gustafson and B. Nilsson-Almqvist, Nucl. Phys. B **281**, 289 (1987).
[53] T. Sjostrand, Comput. Phys. Commun. **82**, 74 (1994).
[54] U. Pettersson, ARIADNE"Lund Preprint LUTP 885, 1988
[55] N. Borghini, P. M. Dinh, J.-Y. Ollitrault, Phys. Rev. C63 (2001) 054906; S. A. Voloshin, A. M. Poskanzer, A. Tang, G. Wang, Phys. Lett. B659 (2008) 537.
[56] A. Bzdak, P. Bozek and L. McLerran, arXiv:1311.7325 [hep-ph].
[57] ATLAS collab, ATLAS-CONF-2014-027, http://cds.cern.ch/record/1702995.
[58] A. Bilandzic, Nucl.Phys.A904-905 2013 (2013) 515c; G. Aad, et al., Phys.Lett. B725 (2013) 60; S. Chatrchyan, et al., Phys.Lett. B724 (2013) 213.